ELSEVIER

Journal of Power Sources 75 (1998) 122–129

JOURNAL OF POWER SOURCES

Electrochemical hydrogen and lithium absorption/desorption in $Ti_{46}Ni_{45}Nb_9$ alloy in aqueous electrolytes

C.S. Wang [a,*], G.T. Wu [b], W.Z. Li [b]

[a] *Department of Materials Science and Engineering, Zhejiang University, Hangzhou 310027, China*
[b] *Department of Physics, Zhejiang University, Hangzhou 310027, China*

Accepted 16 April 1998

Abstract

The electrochemical performance of a $Ti_{46}Ni_{45}Nb_9$ electrode in different solutions has been studied. The $Ti_{46}Ni_{45}Nb_9$ electrode can absorb/desorb hydrogen in 3 M KOH aqueous and lithium in non-aqueous solution (1 M $LiClO_4$ dissolved in a 50/50 vol.% (v/o) mixture of ethylene carbonate and diethyl carbonate), respectively. It is assumed that lithium and hydrogen are incorporated in the $Ti_{46}Ni_{45}Nb_9$ electrode in saturated LiCl + LiOH solution and result in a more positive potential value of hydrogen desorption and an abnormal discharge curve.

Keywords: Hydrogen and lithium storage; Aqueous electrolytes; Electrochemical performance

1. Introduction

In a 1989 review of about 40 battery technologies for electric-vehicle (EV) applications, Ratner et al. [1] concluded that there was no suitable technology currently available for EVs. The review considered factors such as cost, safety, performance, and environmental friendliness. Today, the search for an acceptable EV battery continues. The Ni-metal hydride battery developed by Ovonics (Warren, MI) [2] and aqueous Li-ion battery [3] show promise in the hunt for a suitable EV battery. Thus, we believe that a lithiated-hydride battery in aqueous solution, which can absorb/desorb hydrogen and lithium, may be a good candidate for EVs.

Both hydrogen and lithium can be incorporated in Pd in 0.1 M LiOH solution during the charge/discharge process [3] and the absorbed Li interacts with absorbed hydrogen due to the strong bond between hydrogen and lithium. Partial substitution of Li for Pd increases the amount of dissolved hydrogen and decreases the pressure plateau of hydrogen despite the lattice contraction which occurs on alloying Pd with Li [4]. Unfortunately, no studies on hydrogen and lithium incorporation into AB, AB_2 and AB_5-type hydrogen storage electrodes in aqueous solution have been reported to date. The work presented here has been directed towards a study of the electrochemical performance of hydrogen and lithium insertion/desertion in a hydride electrode in aqueous solution.

Lithium can be intercalated into a host compound from aqueous 1 M LiOH solution only when the potential of the Li intercalated compound is above 2.3 V (vs. Li) [5]. For example, MnO_2 [5] and V_2O_5 [6] are suitable host compounds for lithium intercalation in 1 M LiOH solution. If the activity of water can be reduced, i.e., if hydrogen evolution can be suppressed, a host compound with a potential lower than 2.3 V may intercalate lithium in aqueous solution. The possibility of lithium incorporation with hydrogen into an electrode in aqueous solution is not only dependent on the chemical potential, μ_{Li}^{int}, of intercalated Li and μ_H^{int} of intercalated H in the metal electrode, but also on the relative activity of Li^+ and H_2O in solution [5], for example, both hydrogen and lithium can be intercalated in λ-MnO_2 in aqueous solution, but only lithium is intercalated in a MnO_2 host compound in 1 M LiOH solution [5]. Therefore, the proper relative activities of Li^+, H_2O in solution, μ_{Li}^{int} of intercalated Li, and μ_H^{int} of intercalated H in the metal hydride electrode are needed for the incorporation of hydrogen and lithium.

It has been noted [7] in a work on the solvent extraction of metals that saturated lithium chloride has a high lithium activity and a low free-water activity. In a solution of 13.5

* Corresponding author. Fax: +86-571-795-13-58: E-mail: msecwang@dial.zju.edu.cn

0378-7753/98/$19.00
PII S0378-7753(98)00105-0

M in LiCl, but only 0.1 M in H_2O, most of the water is strongly bound in complexes of the type $Li(H_2O)_n^+$, where $n \approx 4$ [7]. In saturated LiCl/LiOH solution, the reversible potential of the hydrogen electrode (RHE) can be shifted to 1.14 V (i.e., 0.312 V more negative than in conventional solution) and a host compound with a potential above 2.0 V (vs. Li) can intercalate lithium.

We have studied the electrochemical lithium absorption/desorption properties of Mg_2Ni, $Zr(MnVCoNi)_2$, $Mm(NiCoMnTi)_5$, $Ti_1Ni_{0.8}V_{0.2}$ alloy, and $Ti_{46}Ni_{45}Nb_9$ electrodes in non-aqueous electrolytes, and found out that only $Ti_{46}Ni_{45}Nb_9$ and $Ti_1Ni_{0.8}V_{0.2}$ alloys have relative large capacities above 2.0 V vs. Li. In this paper, we have first examined the electrochemical hydrogen and lithium absorption/desorption properties of $Ti_{46}Ni_{45}Nb_9$ electrode in 3 M KOH aqueous solution and in non-aqueous solution (1 M $LiClO_4$ dissolved in ethylene carbonate (EC) and diethyl carbonate (DEC)). Then, a study has been made of hydrogen and lithium incorporation in a $Ti_{46}Ni_{45}Nb_9$ electrode in LiOH aqueous solution and in saturated LiCl + LiOH aqueous solution.

2. Experimental

2.1. Anode electrode

Alloys were prepared by arc melting using starting elements Ti, Ni, and Nb with a purity of 99%, 99.9%, and 99.9%, respectively. The ingots were pulverized into a fine powder (about 300 mesh) by repeated electrochemical absorption/desorption of hydrogen. The electrodes were made by mixing the alloy powder with finely powdered electrolytic copper (300 mesh) at a weight ratio of 1:2. The mixture was cold-pressed into small (inside diameter = 10 mm) copper caps to form test electrodes. Each electrode contained 80 mg active materials. Powder X-ray diffraction (XRD) data were obtained from 300-mesh inactivated alloy powders using a Rigaku C-max-III B diffractometer with CuKα radiation. The composition of each phase was determined by microprobe analysis.

2.2. Electrochemical methods

For the aqueous cells, the electrochemical charge–discharge tests were carried out in an open, standard, three-electrode cell. The counter electrode was nickel hydroxide with much larger total capacity than the $Ti_{46}Ni_{45}Nb_9$ electrode. The reference electrode was Hg/HgO for 3 M KOH and 3 M LiOH solution and Ag/AgCl for saturated KCl + LiOH and 13 M KCl + 3 M KOH solution; the potentials were converted to the Hg/HgO reference potential for comparison. The electrolyte was 3 M KOH, 3 M LiOH, 13 M KCl + 3 M KOH, or saturated LiCl + LiOH solution, as determined by the experimental requirements. The discharge capacities of hydride electrodes were determined by means of a galvanostatic charge–discharge method. To reduce the ohmic drop between the working and reference electrodes, a Lugging capillary was placed close to the hydride electrode. For comparison, Li insertion/desertion in non-aqueous solution was carried out in a sealed three-electrode cell. The $Ti_{46}Ni_{45}Nb_9$ electrode was dried under vacuum at 150°C for 12 h before cell fabrication to avoid possible contamination with water. Li metal foil was used for both the counter and reference electrodes. All procedures for handling and fabricating the cell were performed in an argon-filled glove box. The rest time between the charge and discharge was 6 h. The non-aqueous electrolyte was 1 M $LiClO_4$ dissolved in a 50/50 vol.% (v/o) mixture of EC and DEC. The potential-composition (P-C) curves were measured at a discharge current of 1 mA g^{-1} in 3 M KOH solution and at a discharge current of 0.5 mA g^{-1} in non-aqueous solution. The number of electrons transferred between the two electrodes was calculated from the current, the mass of $Ti_{46}Ni_{45}Nb_9$ and the current duration:

$$\text{electrons}/Ti_{46}Ni_{45}Nb_9 = \frac{QW}{F} = \frac{113.5Q}{26\,800}, \quad (1)$$

where Q is the electrochemical capacity (mAh g^{-1}), F is the Faraday constant (26 800 mAh g^{-1}), and W is the weight per molar $Ti_{46}Ni_{45}Nb_9$ alloy (113.5 g mol^{-1}). The value of electrons/$Ti_{46}Ni_{45}Nb_9$ is equal to the value of $Li/Ti_{46}Ni_{45}Nb_9$ in non-aqueous solution.

3. Results and discussion

3.1. Electrochemical hydrogen desorption properties of $Ti_{46}Ni_{45}Nb_9$ electrode in 3 M KOH solution

The $Ti_{46}Ni_{45}Nb_9$ is composed of three phases: Ti_2Ni, TiNi and a pure Nb, as shown in Fig. 1. Microprobe analysis revealed that part of the Nb was present in TiNi and Ti_2Ni.

Discharge curves and cycle behaviour at a 50 mA g^{-1} discharge current are shown in Fig. 2. The discharge capacity decreases with cycling due to the formation of TiO_2 and Nb_2O_5 on the electrode surface [8]. On the one hand, the oxidation of Ti and Nb decreases the amount of the hydrogen-absorbing element and results in thermodynamic decline. On the other hand, the oxide film increases the discharge polarization, since the oxide film decreases the hydrogen diffusion ability and exchange current [8], and causes a decline in the kinetics.

3.2. Electrochemical lithium absorption / desorption properties of $Ti_{46}Ni_{45}Nb_9$ in non-aqueous solution

The first charge/discharge galvanostatic cycle of a $Ti_{46}Ni_{45}Nb_9$ electrode at a discharge current of 1 mA g^{-1} in non-aqueous electrolyte is shown in Fig. 3. The open-

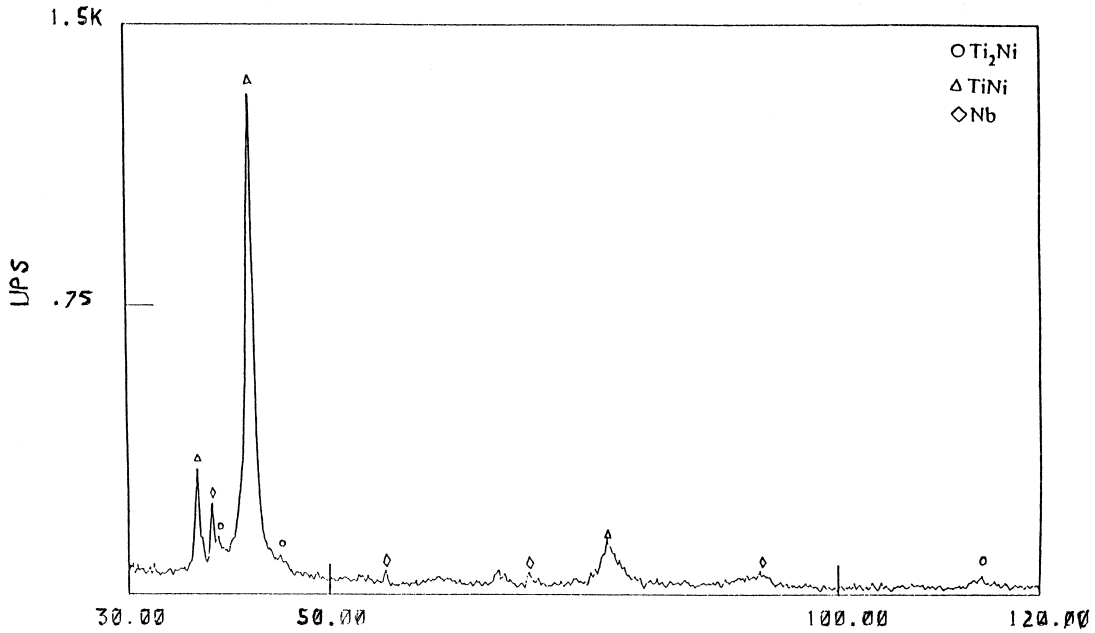

Fig. 1. XRD patterns for $Ti_{46}Ni_{45}Nb_9$.

circuit potential of $Ti_{46}Ni_{45}Nb_9$ is 2.6 V vs. Li. The first charge (Li intercalation) curve reveals clearly a cathodic plateau at a potential of about 1.9 V vs. Li. For discharge (Li extraction), this anodic plateau shifts by up to 2.2 V. The larger potential hysteresis between the charge and discharge may be induced by the lower diffusion coefficient of Li in the $Ti_{46}Ni_{45}Nb_9$ electrode, the thick electrode pellet (1 mm), and some absorption of hydrogen in the $Ti_{46}Ni_{45}Nb_9$ alloy due to the lower pressure the plateau of hydrogen for $Ti_{46}Ni_{45}Nb_9$ alloy (H in carbon can cause a larger potential hysteresis in the charge/discharge process [9]). The slope at 0.8 to ~0.6 V is attributed to the decomposition of the non-aqueous solvent and the formation of a passivation layer on the electrode surface [10].

Fig. 4 presents the variation in capacity and open-circuit potential of a $Ti_{46}Ni_{45}Nb_9$ electrode during charge–discharge cycling in non-aqueous electrolyte. The electrode is

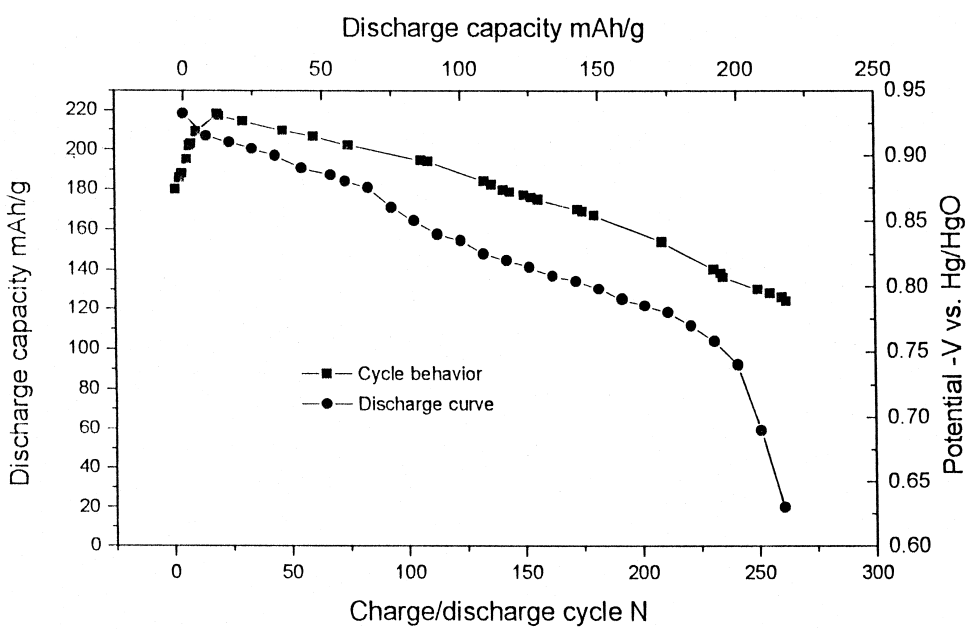

Fig. 2. Discharge curves after activation and cycle behaviour at a discharge current of 50 mA g^{-1}. Before discharge, the electrode was charged at a current density of 50 mA g^{-1} for 6 h.

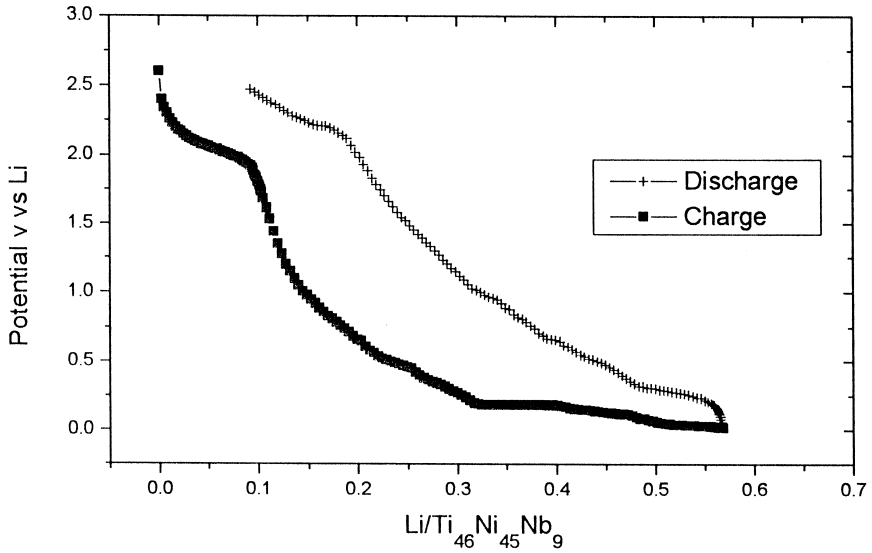

Fig. 3. First charge/discharge galvanostatic cycle of a $Ti_{46}Ni_{45}Nb_9$ electrode in non-aqueous electrolyte at a current density of 1 mA g^{-1}.

cycled over a potential range of 0.01 to 1.5 V and at a current density of 7.5 mA g^{-1}; the rest time between the charge and discharge is 6 h. The data show that the charge capacity decreases and the discharge capacity increases with cycling. This is due to a gradual increase in the lithium remaining in the $Ti_{46}Ni_{45}Nb_9$ electrode, which is induced by the lower diffusion ability of lithium in this electrode. The rate of lithium insertion decreases, but its extraction rate increases with increasing concentration of lithium in the electrode. This can also be confirmed by the variation of the open-circuit potential in the charged and discharged states. Both open-circuit potentials decrease with cycling (see Fig. 4), which means that the residual lithium increases with cycle number. In order to avoid the influence of the state-of-charge, we studied the discharge behaviour of the electrode after short-circuit for 36 h, as shown in Fig. 5. The results showed that with increase in discharge current from 1 to 4 mA g^{-1}, the potential plateau at about 2.2 V move towards a higher potential and the discharge capacity at this plateau potential decreased gradually. This can be explained by the larger electrochemical polarization and concentration polarization at high discharge currents.

3.3. Electrochemical hydrogen and lithium desorption from a $Ti_{46}Ni_{45}Nb_9$ electrode in aqueous solution

In order to identify the possibility of lithium intercalation in aqueous solution, measurement was made of the

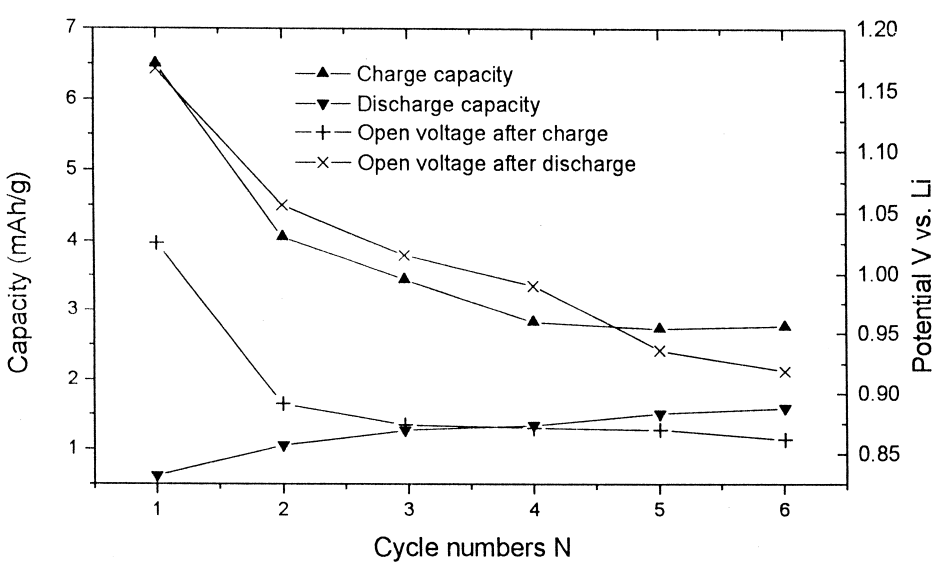

Fig. 4. Capacity and open-circuit potential of a $Ti_{46}Ni_{45}Nb_9$ electrode vs. cycle number in non-aqueous electrolyte. The electrode was cycled over a potential range of 0.01–1.5 V and at 7.5 mA g^{-1}. The rest time between the charge and discharge was 6 h.

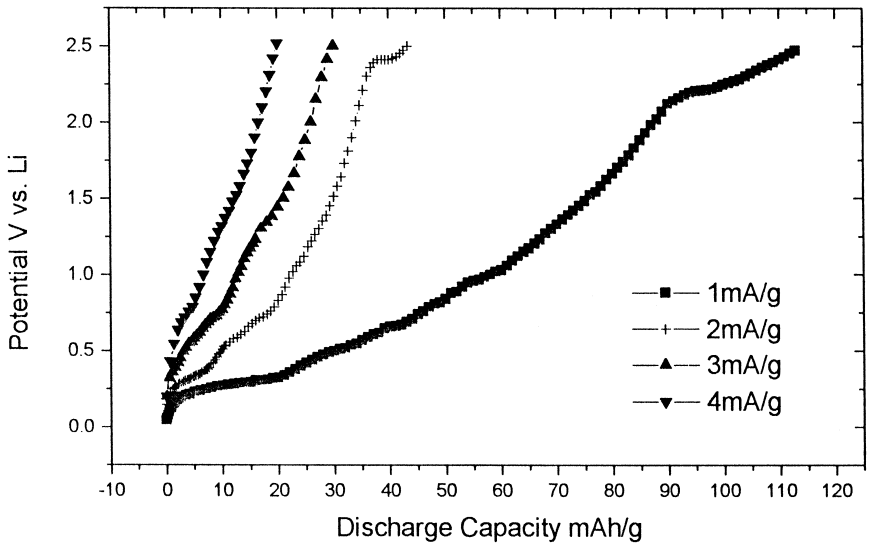

Fig. 5. Discharge curves at different discharge currents. Before discharge, the $Ti_{46}Ni_{45}Nb_9$ electrode was short-circuited for 36 h.

P-C curves of a $Ti_{46}Ni_{45}Nb_9$ electrode in non-aqueous and in 3 M KOH solution. The P-C curves of the $Ti_{46}Ni_{45}Nb_9$ electrode in 3 M KOH and in non-aqueous solution are given in Fig. 6. The measured potential in the non-aqueous solution was adjusted to −3.13 V and referred to Hg/HgO. From the results given in Fig. 6, it can be expected that, in the potential range of the hydrogen absorption reaction (HAR) (−0.923 to ∼ −0.6 V vs. Hg/HgO), only about 0.1 Li/M may intercalate into a $Ti_{46}Ni_{45}Nb_9$ electrode, and if the low kinetics for lithium desorption are considered, the amount of lithium incorporated may be much lower. Also from Fig. 6, it can be concluded that lithium may be incorporated more efficiently in aqueous solution if the hydrogen evolution is suppressed. It has been noted in a work on the solution extraction of metals [11,12] that saturated lithium chloride has a high lithium activity and a low free-water activity. The reversible potential of the lithium electrode in 13.5 M lithium ion solution is −3.13 V vs. Hg/HgO in saturated LiCl, whereas the reversible potential of the hydrogen electrode (RHE) in saturated LiCl is −0.82 V (i.e., 0.3 more negative than in conventional, neutral solution due to the reduced activity of water). Further, the potential of the RHE can shift to −1.22 V if the solution is also saturated with lithium hydroxide (about 3 M) [7]. During the charge process in saturated LiCl + LiOH solution at a current of 50 mA g^{-1},

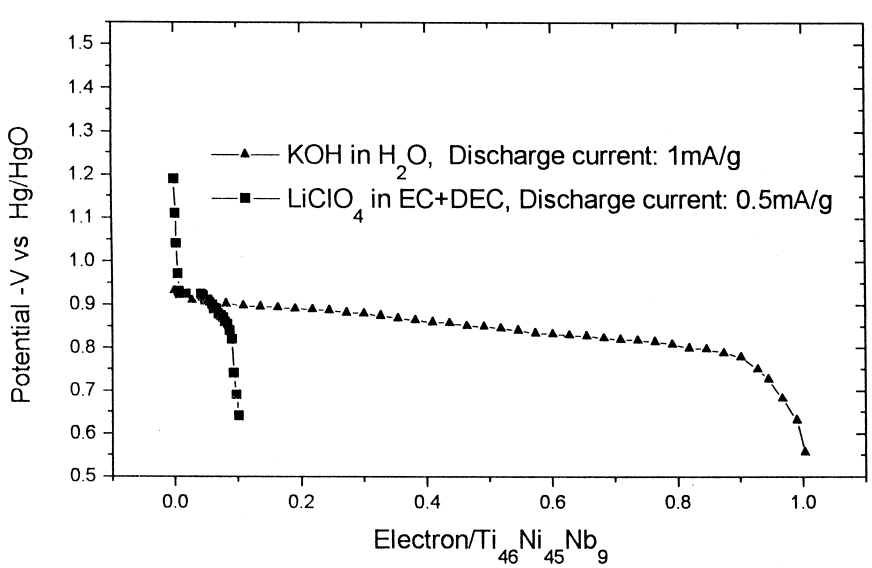

Fig. 6. P-C curves for a $Ti_{46}Ni_{45}Nb_9$ electrode in 3 M KOH and in non-aqueous solution. The measured potential in the non-aqueous solution was adjusted to −3.13 V to refer it to Hg/HgO. Before discharge, the electrode in 3 M KOH was charged at a current density of 50 mA g^{-1} for 6 h.

the potential of $Ti_{46}Ni_{45}Nb_9$ increases gradually and finally reaches −1.2 V (vs. Hg/HgO), a value at which a large amount of hydrogen evolution will occur. It is expected that little lithium is incorporated into a $Ti_{46}Ni_{45}Nb_9$ electrode in 3 M LiOH solution since the discharge behaviour in 3 M KOH is similar to that in 3 M LiOH solution (see Fig. 7). Also from Fig. 7, it can be seen that the discharge potential of the $Ti_{46}Ni_{45}Nb_9$ electrode in saturated LiCl + LiOH solution is more positive than that in LiOH solution and displays an abnormal change in the discharge process, i.e., its discharge potential decreases initially and then increases, but then decreases again. In order to assure that the above phenomena is caused by lithium incorporation with hydrogen in the electrode not by Cl ions, we investigated the discharge characteristics of a $Ti_{46}Ni_{45}Nb_9$ electrode in KCl + KOH with the same concentration as saturated LiCl + LiOH. The results are also shown in Fig. 7. No abnormal potential variation occurs during discharge and the value is lower than in KOH, but higher than in saturated LiCl + LiOH, which indicates that the absorbed lithium in a $Ti_{46}Ni_{45}Nb_9$ electrode moves its potential towards a more positive direction due to the strong bond between the absorbed hydrogen and lithium. This is in agreement with the results reported by Sakamoto et al. [4]. From studies of the hydrogen absorption characteristics of $Pd_{1-x}Li_x$ ($x = 0.05$ and 0.072) alloy and ordered Pd_7Li, these authors concluded that Pd–Li alloys absorb considerable amounts of hydrogen and form a more stable hydride phase than Pd. Thus, absorbed lithium decreases the potential of the hydrogen plateau (vs. Hg/HgO). In Fig. 7, the more rapid decrease in discharge potential of the electrode in KOH + KCl solution than in KOH solution may be induced by the lower free-water activity in the former solution.

The abnormal discharge curves in saturated LiCl + LiOH can also be explained by the strong bond between absorbed lithium and absorbed hydrogen. In the discharge process, both hydrogen and lithium diffuse from the bulk to the surface of the electrode, and then, electrochemical oxidation takes place on the surface. Since absorbed lithium decreases the potential of the $Ti_{46}Ni_{45}Nb_9$ electrode, the potential increases with lithium desorption, but it decreases with desorption of hydrogen (see Fig. 6). The electrode potential is dependent on the amount of residual lithium and hydrogen in the $Ti_{46}Ni_{45}Nb_9$ electrode and the potential change per molar hydrogen and lithium atom. It is logical to expect that the diffusion ability for lithium is much lower than that for hydrogen in a $Ti_{46}Ni_{45}Nb_9$ electrode, because the diffusion coefficient of hydrogen and lithium in TiO_2 are about 10^{-10} to $\sim 10^{-11}$ cm^2 s^{-1} [13] and 9×10^{-14} cm^2 s^{-1} [14], respectively. Thus, hydrogen desorbs more easily than lithium at a certain discharge condition. Also, the potential decline per molar hydrogen changes with the discharge state. At initial and final discharge states, the potential drop per hydrogen atom is fast, but in the middle of the discharge process, the potential decreases gradually according to the discharge curve in 3 M KOH solution (Fig. 7). Consequently, when the electrode discharges in saturated LiCl + LiOH, the fast potential drop during the initial discharge process is due mainly to the fast desorption rate of hydrogen, the slow desorption rate of lithium, and the large potential decline per hydrogen atom. The subsequent rise in potential may be caused by the smaller potential decline per molar hydrogen in the middle of the discharge process and the gradual desorption of lithium. As we have described, the potential plateau of lithium desorption in non-aqueous solution at about 2.2 V moves towards a higher potential

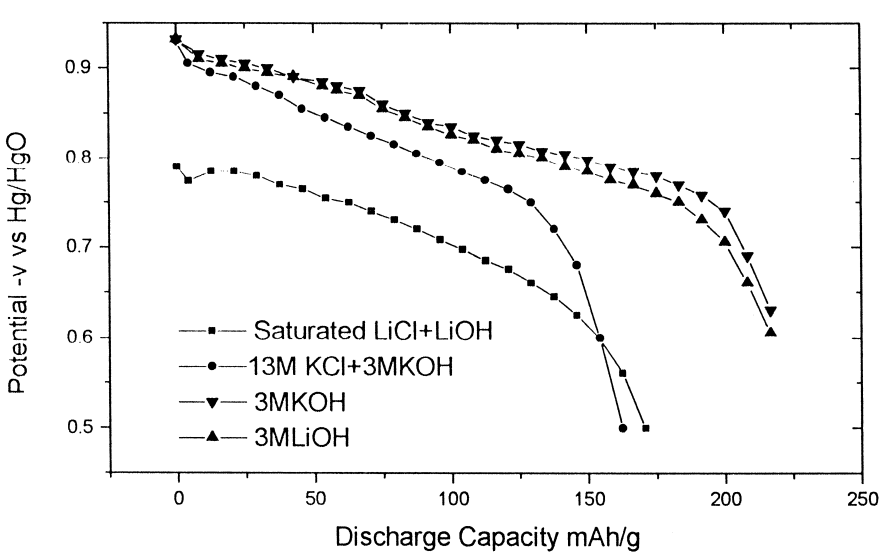

Fig. 7. Discharge curves for a $Ti_{46}Ni_{45}Nb_9$ electrode in 3 M KOH, 3 M LiOH, 13 M KCl + 3 M KOH and saturated LiCl + LiOH solution with a discharge current of 50 mA g^{-1}. Before discharge, the electrode was charged at a current density of 50 mA g^{-1} for 6 h.

and the discharge capacity at this plateau potential decreases gradually with increase in discharge current from 1 to 4 mA g^{-1} (Fig. 5). Therefore, the lithium desorbed would decrease with increase in discharge current when the electrode discharges in saturated LiCl + LiOH, and the amplitude of the rising potential decreases with increase in discharge current.

In order to confirm the above analysis, an investigation was made of the discharge process of a $Ti_{46}Ni_{45}Nb_9$ electrode in saturated LiCl + LiOH at different discharge currents and certain charge conditions. The results are presented in Fig. 8. As expected, the amplitude of the potential rise decreases with increase in discharge current, and when the discharge current density is at 1 mA g^{-1}, the discharge potential rises abruptly at the end of discharge. The rapid increase in potential suggests that almost all of the absorbed lithium and hydrogen in the $Ti_{46}Ni_{45}Nb_9$ electrode is desorbed at a discharge current density of 1 mA g^{-1} [15]. Therefore, the amount of absorbed lithium and hydrogen can be determined from the discharge capacity of the $Ti_{46}Ni_{45}Nb_9$ electrode at a low discharge current density of 1 mA g^{-1}. The discharge capacity of a $Ti_{46}Ni_{45}Nb_9$ electrode in saturated LiCl + LiOH at a discharge current density of 1 mA g^{-1} is 280 mAh g^{-1}, which corresponds to a content of 1.2 (H + Li)/$Ti_{46}Ni_{45}Nb_9$ according to Eq. (1). From Fig. 6, it can be seen that the content of absorbed hydrogen in KOH solution at a discharge current density of 1 mA g^{-1} is 1 H/$Ti_{46}Ni_{45}Nb_9$. Therefore, the amount of incorporation of lithium in a $Ti_{46}Ni_{45}Nb_9$ alloy is calculated to be 0.2 Li/$Ti_{46}Ni_{45}Nb_9$. In the present study, all the $Ti_{46}Ni_{45}Nb_9$ electrodes in aqueous solution were charged at a current density of 50 mA g^{-1} for 6 h (corresponding to 1.27 electrons/$Ti_{46}Ni_{45}Nb_9$) before discharge, but only 1 H/$Ti_{46}Ni_{45}Nb_9$ was inserted in electrodes in KOH, LiOH and 13 M KCl + 3 M KOH solutions, and 1.2 (H + Li)/$Ti_{46}Ni_{45}Nb_9$ was simultaneously inserted in the electrode in saturated LiCl + LiOH solution due to the hydrogen evolution reaction.

The results of this initial study are very promising and suggest that the $Ti_{46}Ni_{45}Nb_9$ electrode can be used as a hydrogen and a lithium storage material. Also, nickel hydroxide can absorb/desorb hydrogen and lithium in KOH + LiOH solution [16]. Thus, a $Ni(O(HLi))_2/Ti_{46}Ni_{45}Nb_9(LiH)_x$ system can be fabricated as a new kind of rechargeable lithiated-hydride cell. The drawbacks of $Ti_{46}Ni_{45}Nb_9$ electrode at present are: (i) lower capacity partly due to the suppressing effects for water activity by LiCl, and (ii) the small amount of absorb/desorb lithium in the charge/discharge process. These problems can be ameliorated by two methods. One is seeking other kinds of hydride electrode materials which have larger lithium absorption/desorption capacity at potentials above 2.2 V vs. Li. We believe that the materials with more bound lithium atoms and with a layered-structure may be good candidates for lithiated-hydride electrode materials. We also have tested Mg_2Ni, $Zr(MnVCoNi)_2$, and $Mm(NiCoMnTi)_5$ and $Ti_1Ni_{0.8}V_{0.2}$ alloys; only $Ti_1Ni_{0.8}V_{0.2}$ alloy is promising. The experimental results for the $Ti_1Ni_{0.8}V_{0.2}$ electrode are ready for publication. The second method is to use a partial substitution method to adjust the insertion/desertion potential of lithium and hydrogen in a LiOH electrolyte. In LiOH solution, the $M(LiH)_x$ electrode may be expected to have better cycle

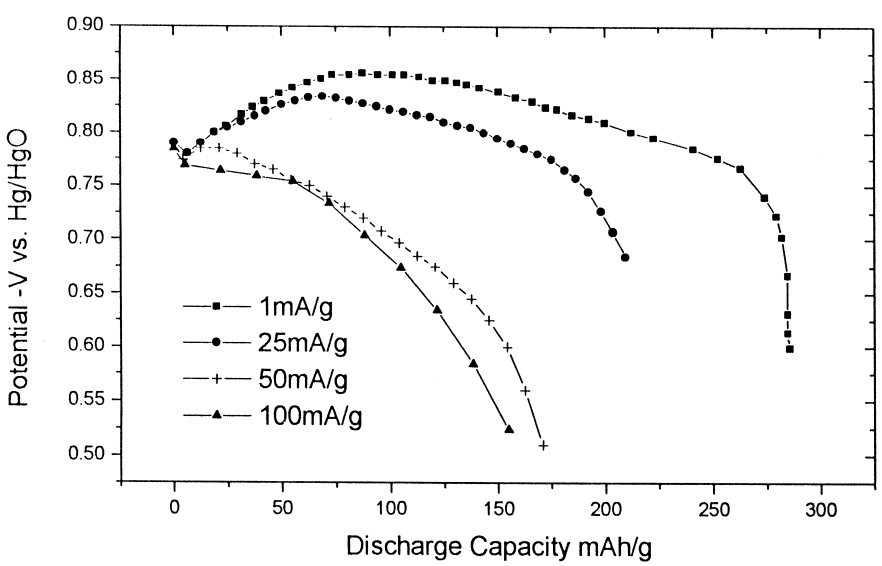

Fig. 8. Discharge curves for a $Ti_{46}Ni_{45}Nb_9$ electrode in saturated LiCl + LiOH at different discharge currents. Before discharge, the electrode was charged at a current density of 50 mA g^{-1} for 6 h.

life due to the excellent electrical conductivity of the lithiated oxide film formed on the electrode surface [16]. The research on this system is in progress.

4. Conclusions

A $Ti_{46}Ni_{45}Nb_9$ hydride electrode can absorb large amounts of hydrogen in 3 M KOH solution. At a discharge current of 50 mA g^{-1}, its discharge capacity is 220 mAh g^{-1}. After 250 charge/discharge cycles at this current, the discharge capacity drops to 130 mAh g^{-1}. Also, the $Ti_{46}Ni_{45}Nb_9$ electrode can absorb/desorb about 0.5 M Li per molar $Ti_{46}Ni_{45}Nb_9$ at a discharge current of 1 mA g^{-1} in non-aqueous solution. The electrode may absorb/desorb about 0.1 M Li at a potential between 2.1 and 2.5 V vs. Li (the water stability window for 3 M KOH solution) according to the P-C curves for a $Ti_{46}Ni_{45}Nb_9$ electrode in non-aqueous solution. Lithium does not incorporate in a $Ti_{46}Ni_{45}Nb_9$ electrode in 3 M LiOH solution, which may be due to the higher relative activity of H_2O and the lower relative activity of Li^+ in 3 M LiOH solution. In saturated LiCl + LiOH solution, however, the lithium presumed to be incorporated in a $Ti_{46}Ni_{45}Nb_9$ electrode has an influence on the discharge curves, as a result of the lower potential of hydrogen desorption and the occurrence of an abnormal discharge curve. The latter can be explained by the strong interaction between absorbed lithium and absorbed hydrogen in the $Ti_{46}Ni_{45}Nb_9$ electrode and the higher diffusion ability of hydrogen compared with that of lithium.

Acknowledgements

The authors acknowledge the financial support from the National Natural Science Foundation of China (No. 59502005).

References

[1] E.Z. Ratner, P.C. Symons, W. Walsh, C.J. Warde, G.L. Hendriksen, Assessment of battery technologies for electric vehicles, Contract DE-AC07-761DO1570, U.S. Dept of Energy, Washington, DC, August 1989.
[2] S.R. Ovshinsky, M.A. Fetcenko, J. Ross, Science 260 (1993) 176.
[3] A. Czerwinski, R. Marassi, J. Electroanal. Chem. 323 (1992) 373.
[4] Y. Sakamoto, T. Hisamoto, M. Ura, R. Nakamura, J. Alloys Comp. 200 (1993) 141.
[5] W. Li, W.R. McKinnon, J.R. Dahn, J. Electrochem. Soc. 143 (1996) 2730.
[6] M.J. Zhang, J.R. Dahn, J. Electrochem. Soc. 143 (1996) 2730.
[7] R.L. Deutscher, T.M. Florence, R. Woods, J. Power Sources 55 (1995) 41.
[8] C.S. Wang, Y.Q. Lei, Q.D. Wang, J. Power Sources, in press.
[9] Tao Zheng, W.R. McKinnon, J.R. Dahn, J. Electrochem. Soc. 143 (1996) 2137.
[10] G.B. Appetecchi, F. Croce, J. Power Sources 51 (1994) 79.
[11] T.M. Florence, Y.T. Farrar, Anal. Chem. 41 (1968) 1200.
[12] T.M. Florence, Y.T. Farrar, Aust. J. Chem. 22 (1968) 473.
[13] Young Yoon, Su-Il Prun, Electrochim. Acta 40 (1995) 999.
[14] M.P. Cantao, J.I. Cisneros, R.M. Torres, J. Phys. Chem. 98 (1994) 4865.
[15] T. Nohira, Y. Ito, J. Electrochem. Soc. 144 (1997) 2290.
[16] Varta Batteries, Sealed Nickel/Cadmium Batteries, 1982.